Particle Deposition, Transport and Fuelling in Pellet Injection Experiments at JET

D. Frigione[1], L. Garzotti[2], E. Giovannozzi[1], F. Köchl[3], P. T. Lang[4], B. Alper[2], E. Belonohy[5], A. Boboc[2], K. Gál[5], G. Kocsis[5], Y. Liang[6] and JET-EFDA contributors*

JET-EFDA, Culham Science Centre, OX14 3DB, Abingdon, OXON, UK

1. Associazione EURATOM-ENEA sulla Fusione, CP 65, Frascati, Rome, Italy
2. Euratom/CCFEA Fusion Association, Culham Science Centre, Abingdon, OX14 3DB, UK
3. Association EURATOM-ÖAW/ATI, Atominstitut, TU Wien, 1020 Vienna, Austria
4. MPI für Plasmaphysik, EURATOM Association., Boltzmannstr. 2, 85748 Garching, Germany
5. KFKI RMKI, EURATOM Association, P.O.Box 49, H-1525 Budapest-114, Hungary
6. Forschungszentrum Jülich GmbH, Institut für Plasmaphysik, EURATOM-Assoziation, Trilateral Euregio Cluster, D-52425 Juelich, Germany
* See the Appendix of F.Romanelli et al., Fusion Energy (Proc. 22nd Int. Conf. Chengdu) IAEA, 2008

Abstract

Pellet ablation and particle deposition have been extensively studied at JET giving a clear evidence of ∇B drift effects in hot plasmas and its impact on fuelling efficiency. This result confirms observations made on smaller devices. In L-mode or moderately heated H-mode this effect seems to be weak while at high temperature, injection from the VHFS has proven to be much more effective than from LFS in depositing particles beyond the pedestal. In the latter case ablated particles are quickly lost due to a combination of ∇B drift and edge instabilities. The fuelling performance, although investigated only in a limited range of plasma and pellet parameters, seems to be promising for the capability of pellets to raise the density without increasing the neutral pressure in the main chamber. This latter feature is important for ITER, because it confirms that pellets are less demanding in terms of required pumping speed. Experiments of pellet fuelling in combination with ELM mitigation techniques using Error Field Correction Coils (EFCC) have also given encouraging results and are also reported.

1. Introduction

Fuelling of reactor grade plasmas will become more critical than in existing Tokamaks due to high edge plasma temperatures that limit the penetration of neutral particles from the edge. Pellet injection is expected to become the routine tool for overcoming this problem. The viability and the efficiency of this method need to be further investigated in large tokamaks in order to gain confidence in extrapolation to ITER. Several pellet injection experiments have been performed at JET using different injection lines [1,2,3]. This paper reports a detailed analysis of the most recent results obtained with the High Frequency Pellet Injector (HFPI) installed at JET for fuelling and ELM pacing purposes using a Low Field Side (LFS) and a Vertical High Field Side (VHFS) injection lines. This work will concentrate on the particle deposition and density profile evolution following the injection of fuelling pellets. The ELM pacing investigations are reported in other contributions to this conference [4 and refs therein]

The new pellet launcher [5] has been able to deliver continuous pellet trains through the LFS track producing a quasi-stationary two-fold density increase in L-mode and a 25% increase in H-mode baseline scenario. Intact large pellets reach the plasma up to a speed of 200 m/s and a repetition rate up to 10 Hz. Although a significant improvement is still needed to reduce transfer losses through the VHFS line (only one pellet out of three reaches the

plasma, while LFS is better than 90%) available data allowed to perform a detailed study of ablation, deposition and transport.

2. Experimental Set-up

The results described in this paper were obtained using a variety of plasma parameters with plasma current ranging from 2.0 to 2.5 MA, toroidal field between 2.2 and 2.7 T and additional heating power from 5 to 21 MW, mainly provided by Neutral Beam Injection (NBI). Both high (δ_{up}=0.42, δ_{low}=0.40) and low (δ_{up}=0.18, δ_{low}=0.35) triangularity shapes were used with different strike point positions for varying divertor pumping capability. L-mode, base-line H-modes and Hybrid regimes were explored. The full Carbon wall was frequently covered with a beryllium layer deposited by overnight Be-evaporation to
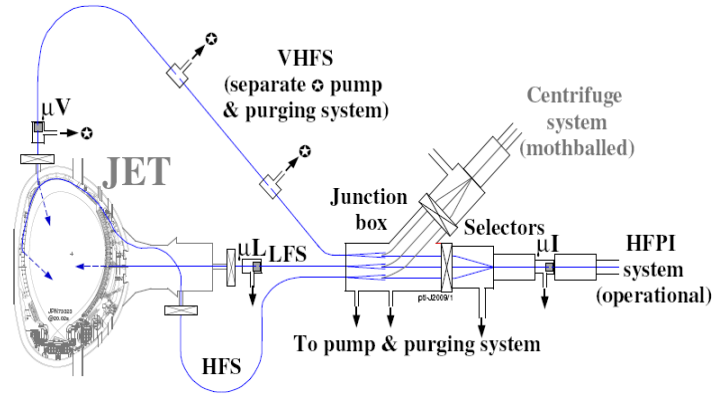

FIG. 1. Schematic of the pellet injection system.

reduce Oxygen content. The divertor structure illustrated in fig 2, could bear power on the central tile, replacing the old septum, thus allowing high triangularity operation.

Deuterium pellets were produced by the new injector (HFPI) [5] designed and built by PELIN laboratory (Russia) on the basis of a previous device installed and successfully tested on Tore Supra [6] . A schematic of the pellet injection system is shown in Fig. 1. The design pellet parameters for fuelling pellets were 35-70 mm^3 volume, corresponding to 2.2-3.8 x 10^{21} D atoms, 100-500 m/s speed, up to 15 Hz repetition rate. In the cases considered here, the pellet speed was in the range 180-200 m/s, the nominal mass was of the order of 3×10^{21} Deuterium atoms and a frequency up to 10 Hz. Deuterium ice was produced by a screw extruder as a continuous string which is then cut in small cylindrical pieces accelerated by a short pulse of helium propellant gas. Via a selector, pellets can be routed along three different tracks corresponding to the injection lines illustrated in fig.2 together with a typical JET magnetic field configuration. Only low field side (LFS) and vertical high field side (VHFS) lines have been used in the present experiments, the HFS one not having been commissioned yet for operation on plasma. Four microwave cavities could measure the pellet mass at various locations.. Two of them, one calibrated to detect large fuelling pellets and the other one for
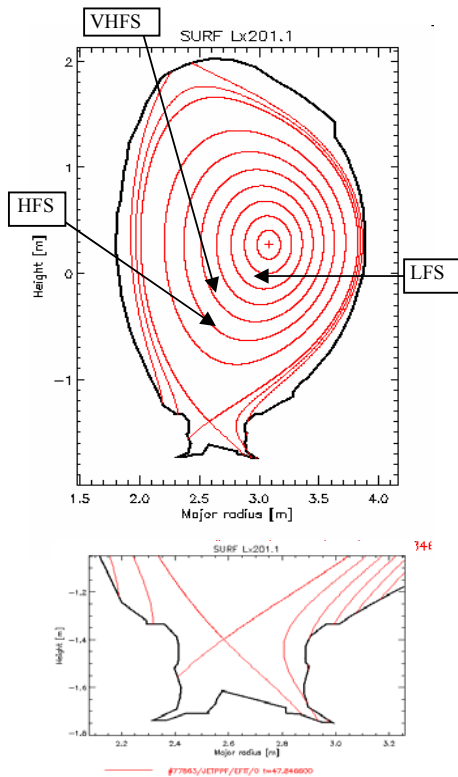

FIG. 2 .Top: JET plasma geometry and aims of pellet injection trajectories. Bottom:details of the Divertor field lines

smaller pacing pellets, were placed just at the injector output. Then one other cavity, calibrated for fuelling pellets, was located at the end of the VHFS line, and one, for pacing pellets, at the end of the LFS track..

A High Resolution Thomson Scattering system (HRTS) with 20 Hz repetition rate and 50 detection points along a horizontal chord, was used to measure the electron density and temperature profiles. It was not possible to synchronize pellets with individual laser pulses, but, in some cases, HRTS profiles were available a few ms after pellet injection thus giving the chance of measuring the pellet particle deposition before any diffusive process could take place. Density profiles were also measured by an eight chord DCN laser interferometer (λ = 195µm). The interferometer could routinely yield a profile every 5ms by inversion of the line integrated data, after the correction of fringe jumps caused by the pellet injection itself. These corrections were also cross-checked with the TS profiles whenever a TS pulse was present between two successive pellets.

In regard to D_α light associated with the ablation process, a set of diodes was available to view VHFS pellets as well as a fast camera viewing the full LFS pellet path. A slow camera was also able to observe the final part of the VHFS pellet trajectory.

3. Particle Deposition

As mentioned before, an accurate measurement of the pellet particle deposition was possible when a HRTS laser shot happened a few ms after the pellet ablation. In these cases, observations should not be affected by diffusive transport phenomena taking place on a longer time scale. With this criterion we have selected a few shots which were the most representative of L-mode, moderately heated (~10 MW) H-mode and high power (~21 MW) Hybrid plasmas. Figure 3 shows the density and temperature profiles before and after the pellets in the three cases both for LFS and VHFS injection. The top row refers to L-mode, the middle row to H-mode and the bottom row to the Hybrid. In L-mode (P_{NBI}~5 MW) and moderately heated H-mode (P_{NBI}~10 MW) both LFS (#76411) and VHFS (#76570) pellets deposit particles inside the separatrix and show little differences between the two tracks. At higher heating power, in the hybrid discharge heated with about 21 MW of NBI, pellets injected from the LFS became very ineffective in depositing particles in the core plasma resulting in an almost unchanged density profile while VHFS pellets were able to produce a clear particle deposition beyond the separatrix. This observation confirms the impact of the pellet injection geometry with respect to the magnetic field gradient on the fuelling capability of the system. As shown later on, an integrated ablation/drift code gives a quantitative account of this observation in terms of ∇B radial particle drift. Of course, this advantage, given by the physics of ablation and particle displacement, has a counter part in the technical difficulties of transferring and injecting pellets from the VHFS.

In L-mode, the line average density jump provoked by the pellet, as measured by the central chord, decays to half its initial value within $\tau_{1/2}$ ~ 0.3 s which is in the range of a purely diffusive process. In the moderately heated H-mode the density decay is much faster ($\tau_{1/2}$ ~ 0.05 s). This is interpreted as due to a more peripheral deposition, due to the existence of a hot pedestal, and the effect of ELMs, either spontaneous or triggered by pellets, which rapidly flush out the extra particles from the pedestal zone. This observation stresses once more the importance of effectively depositing particles beyond the pedestal in order to avoid the fast losses provoked by the ELM crashes. The third case, the hybrid H-mode heated with 21 MW of NBI, shows a decay similar to the H-mode when pellets are injected from the VHFS while, as already mentioned, the density jump and its decay in the LFS case, if any, is within the noise level hence, not measurable.
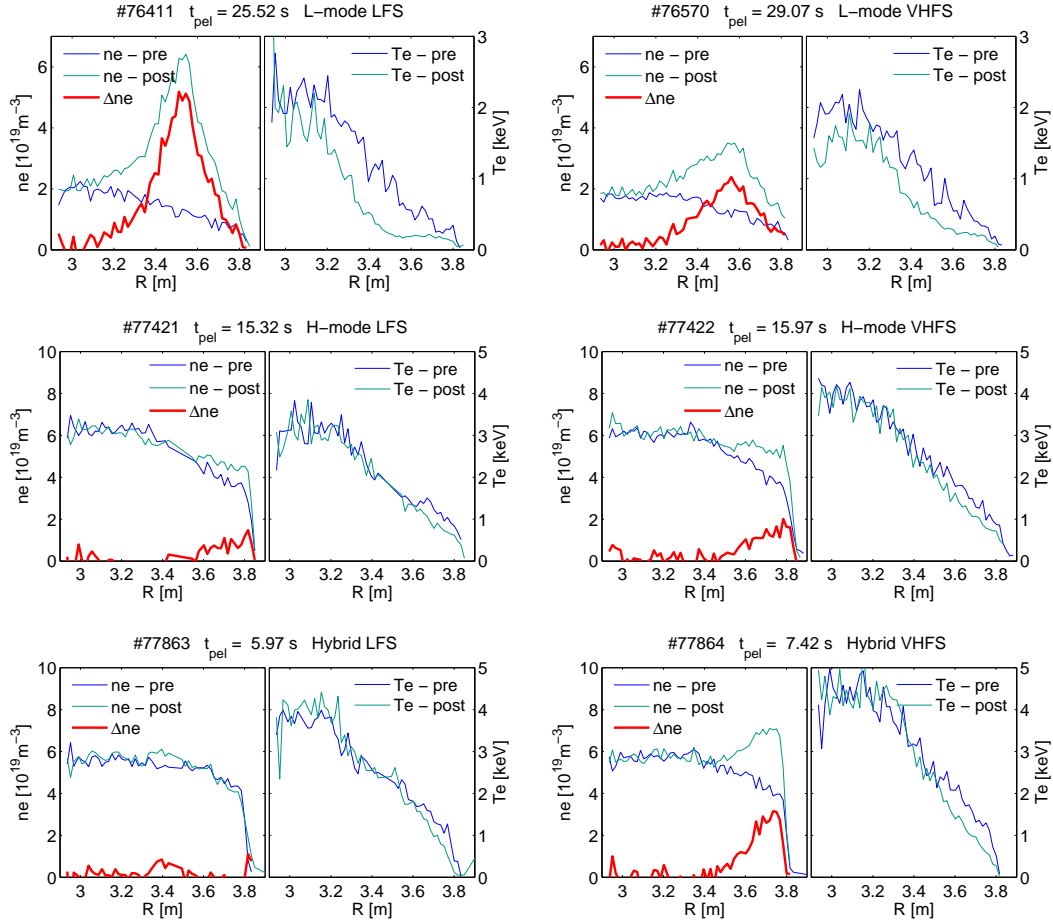
FIG. 3. Density and temperature profiles before and immediately after pellet injection as measured by the Thomson Scattering. Particle deposition (n_{post}-n_{pre}) is also shown in the density box/ Top: L-mode (5 MW); Middle: H-mode(10 MW); Bottom: Hybrid (21

4. Ablation and ∇B Drift

Particular attention was paid to investigate the effect of the radial particle drift predicted by the theory [7] and already observed on medium size tokamaks such as ASDEX-Upgrade, DIII-D, FTU and MAST [8-11]. In the first two cases of section 3, i.e. L-mode and moderately heated H-mode, the particle deposition, as measured by the HRTS is consistent, within experimental errors, with ablation simulations performed with a pure NGPS ablation code not including drift effects. This is shown in FIG. 4 where the experimental particle deposition is compared with code simulations without any drift effect. The code reproduces the fact that there is little difference between LFS and VHFS injection in terms of particle deposition. In L-mode, which is not affected by ELMs, there seems to be some outward displacement in the LFS case and some inward displacement in the VHFS one with respect to ablation predictions (fig.4). In H-mode, the density signal is far too noisy to reveal a possible effect of this kind.

The third case (Hybrid, 21 MW), in presence of a higher temperature pedestal, radial ∇B drift effects need to be included to explain the different fuelling efficiency observed between the two tracks. As already pointed out, in this case the effect of the ∇B drift is dramatic making pellets injected from the LFS, in the available speed range, unable to deposit particles in the core plasma. When injected from LFS, particles are rapidly displaced outwards and then lost via edge instabilities. On the contrary, when injected from the VHFS similar pellets deposit particles beyond the pedestal, as documented by the HRTS profiles and then are retained in the main plasma.. Ablation and deposition simulations including drift effects are shown in FIG. 5. These simulations were performed within the JINTRAC code suite using JETTO as a core transport code and HPI2 for pellet ablation and ∇B drift effect calculations [12-14]. Particles injected from the VHFS although ablated more peripherally than those from LFS (red curves) due to different aim lines, are then displaced inward when the drift effect is included while those from LFS are shifted towards the extreme periphery. The reason why the latter do not appear at all in the plasma after few ms is possibly due to ELM losses.
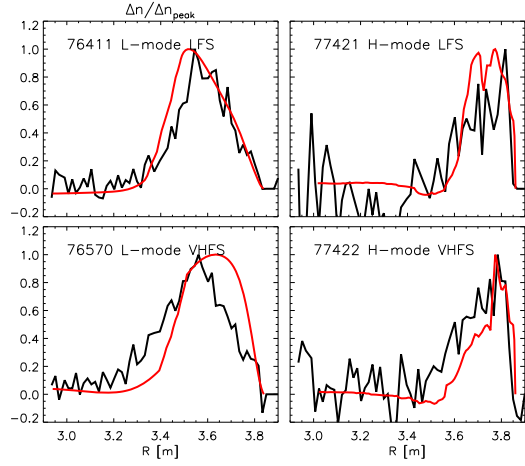

FIG. 4. Experimental particle deposition compared with simulations performed with HPI2 with zero ∇B drift (red) Particles injected from VHFS show a moderate inward drift.
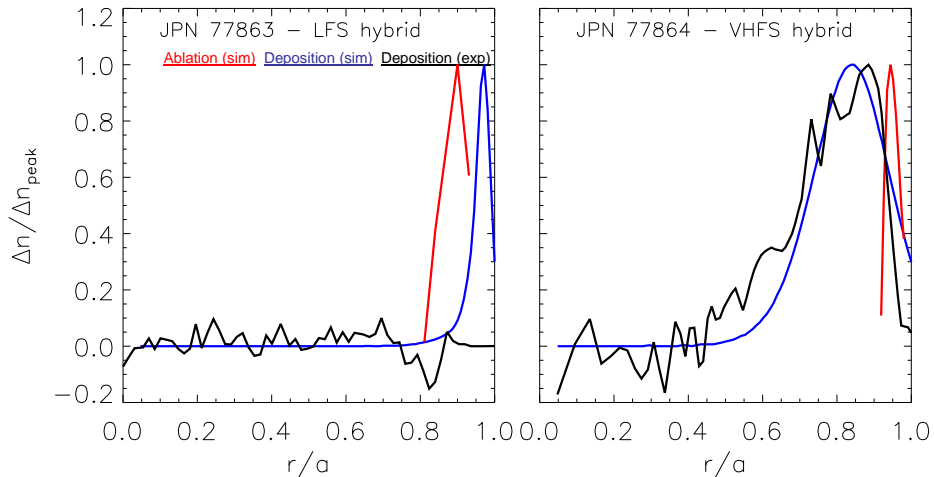

FIG.5. Simulations with HPI2 show a clear effect of ∇B drift on pellets injected from the LFS (left) and VHFS (right) into high power (~21 MW) hybrid discharges. Particles injected from LFS are rapidly displaced outwards and leave the main plasma, while in the VHFS case they are shifted inwards producing a significant modification of the density profile.

5. Particle Diffusion

The particle transport was also analysed on a longer time scale. As already pointed out, the post pellet density decay time shows a significant difference between L-mode and H-mode plasmas. In the latter case, injected particles are lost more quickly ($\tau_{1/2} \sim$ 0.05 s) while in L-mode they are retained for longer ($\tau_{1/2} \sim$ 0.30 s). A more peripheral deposition, due to the hot pedestal and the presence of ELMs contribute to the faster decay in H-mode. An analysis of the post-pellet density profile evolution shows a diffusive process with a diffusion coefficient well described by the Bohm-gyro-Bohm (BgB) law with an anomalous enhancement factor of the order 3-8 in the pellet deposition zone. In absolute numbers, the peripheral diffusion coefficient is reduced in the post pellet phase as shown in fig 6 and 7 for all the cases. Nevertheless, the reduction is smaller than what predicted by the BgB after the density increase. Such a relative degradation with respect to BgB is attributed to turbulence induced by the pellet perturbation. No inward pinch was observed as it is expected at these high collisionalities.
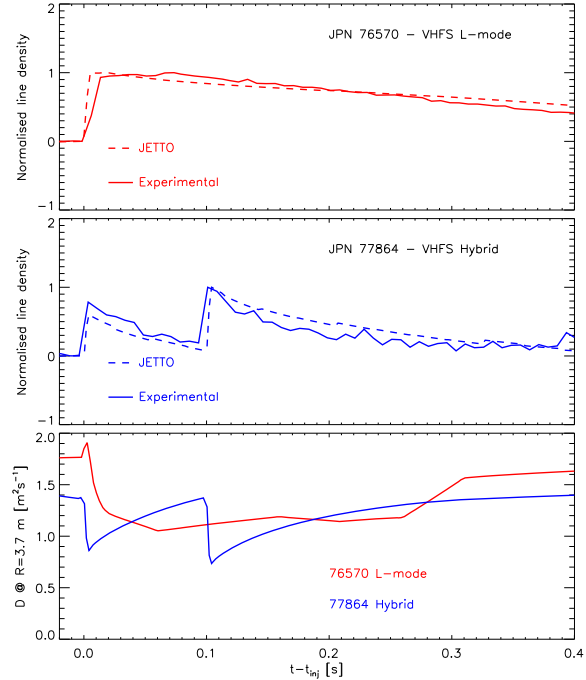

FIG.6. The post pellet line density evolution is well reproduced by JETTO simulations using a BgB diffusion coefficient (bottom) with an enhanced factor of 3-8 in the pellet deposition zone.
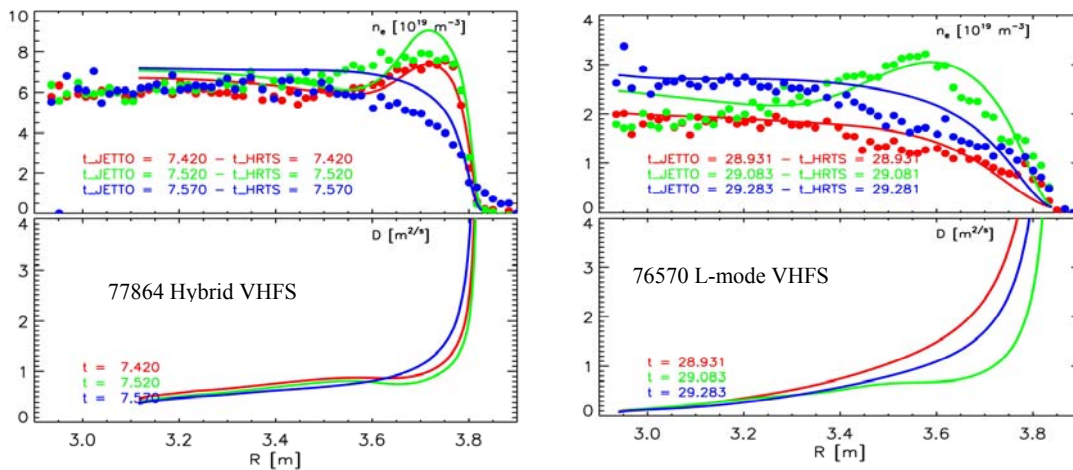

FIG. 7. Experimental density profiles compared with simulations. In the bottom boxes, the corresponding profiles of the particle diffusion coefficients are shown

6. Fuelling

The investigation of the steady state fuelling performance, requiring repetitive injection at several Hz, was mainly restricted, to the LFS track. Indeed, in terms of transmission efficiency, the VHFS track was much worse than LFS especially when going to higher frequencies. Both in L-mode and moderately heated H-mode the fuelling effect was visible as a steady increase of the line average density. In H-mode, the increase of the density was accompanied by some confinement deterioration as it is observed also when trying to increase the density with gas puffing. In the hybrid, which responded only to VHFS pellets, it was not possible to see any steady fuelling effect. Figure 8. shows, for an L-mode and an H-mode, the divertor neutral density, the gas puffing rate and the central line density during a pellet fuelling experiment. As it is shown, pellets show the advantage of giving a negligible contribution to the neutral pressure in the vessel thus being promising for meeting pumping limitations in ITER [15]
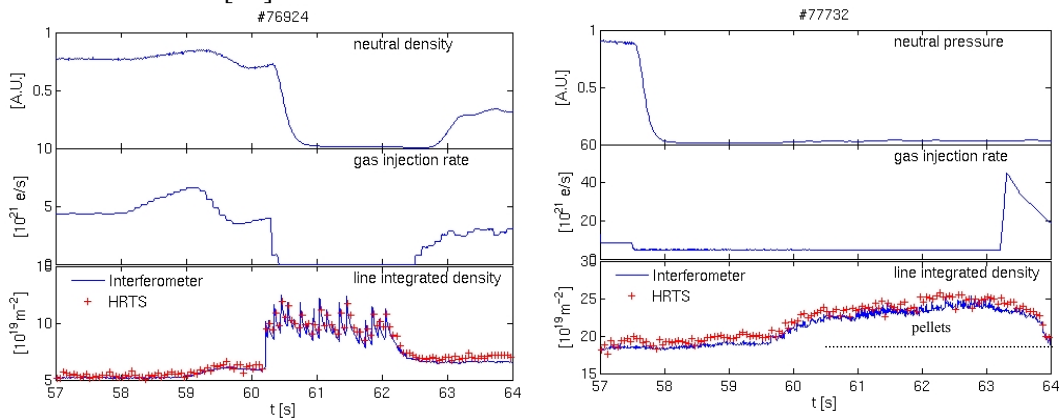

FIG. 8. Divertor neutral density, gas injection rate and central line average electron density during the injection of a 5 Hz pellet train in L (left) and H (right) mode.
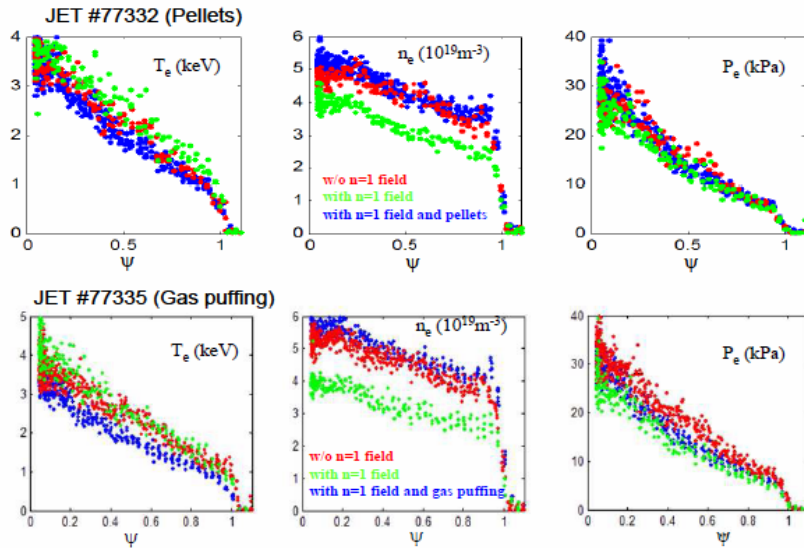

FIG. 9. Electron temperature, density and pressure profiles before and during ELM mitigation experiments with resonant magnetic perturbation (n=1)..The density pump-out is compensated by pellets (top row) or by gas fuelling (bottom row). (Liang)

Pellets were also injected during ELM mitigation experiments performed applying n=1 external magnetic field perturbations in low triangularity plasma. As already documented, a density pump-out effect is observed during the application of the external fields which leads to a drop of the pedestal density. For compensating such a drop, both gas and pellet fuelling were used. In fig 9 [16,17] radial profiles of electron and density temperatures are shown for the two cases together with the corresponding profiles in the phases without and with the external fields. In addition to a smaller impact on the neutral pressure, pellets performed better than gas allowing a full recovery of the reference plasma pressure.

7. Conclusions

Pellet ablation and particle deposition have been extensively studied at JET giving a clear evidence of ∇B drift effect in hot plasmas. In L-mode or moderately heated H-mode this effect seems to be weak. At high heating power, injection from the VHFS has proven to be much more effective than from LFS in depositing particles beyond the pedestal. In the latter case ablated particles are quickly lost due to a combination of ∇B drift and edge instabilities. The fuelling performance, although investigated only in a limited range of plasma and pellet parameters, seems to be promising for the capability of pellets to raise the density without increasing the neutral pressure in the main chamber. This latter feature is important for ITER, because confirms that pellets are less demanding in terms of pumping capabilities.

References

1.   Jones T.T.C. et al. 27th EPS Conf. on PPCP, Budapest, June 2000 ECA Vol 24B
2.   Lang P.T et al. Nucl. Fusion 42 (2002) 388–402
3.   Frigione D et al., 36th EPS Conf, on PPCF, Sofia, June 2009 ECA Vol.33E
4.   Lang P.T. et al. ELM pacing, JET, this conference
5.   Geraud A. et al., Fusion Engineering and Design 69 (2003) 5
6.   Geraud A. et al. Journal of Nuclear Materials 337–339 (2005) 485–489
7.   Rozhansky V. et al., PlasmaPhys. Control. Fusion 37 (1995) 399-414
8.   Lang P.T. et al., Phys. Rev. Letters 79 (1997) 1487- 1490
9.   Baylor L.R. et al., Nucl. Fusion 47 (2007) 1598–1606
10.   Terranova D. et al. Nucl. Fusion 47(2007) 288
11.   Valovic M. at al. Journal of Physics: Conference Series 123 (2008) 012039
12.   Garzotti L. et al 1997 Nucl. Fusion 37 1167
13.   Pégourié B et al., Nucl. Fusion 47 (2007) 44-56
14.   Koechl F., 37th EPS Conf, on PPCF, Dublin, June 2009, paper 04.123
15.   ITER Physics Exper Groups, Nuclear Fusion, Vol. 39, No. 12
16.   Liang Y, et al 2007, Phys. Rev. Lett. 98, 265004 (2007)
17.   Liang Y. et al , Proceedings of ITC19, 2009, accepted for publication in Plasma and Fusion Researh (2010)